Video Article

AFM and Microrheology in the Zebrafish Embryo Yolk Cell

Maria Marsal[1], Ignasi Jorba[2], Elena Rebollo[1], Tomas Luque[2], Daniel Navajas[2], Enrique Martín-Blanco[1]

[1]Instituto de Biología Molecular de Barcelona, Consejo Superior de Investigaciones Científicas

[2]Institute for Bioengineering of Catalonia, Universitat de Barcelona and CIBER Enfermedades Respiratorias

Correspondence to: Enrique Martín-Blanco at embbmc@ibmb.csic.es

URL: https://www.jove.com/video/56224
DOI: doi:10.3791/56224

Keywords: Developmental Biology, Issue 129, Zebrafish, Yolk, Atomic Force Microscopy, Cortical Tension, Microrheology, Nanoparticle tracking

Date Published: 11/29/2017

Citation: Marsal, M., Jorba, I., Rebollo, E., Luque, T., Navajas, D., Martín-Blanco, E. AFM and Microrheology in the Zebrafish Embryo Yolk Cell. *J. Vis. Exp.* (129), e56224, doi:10.3791/56224 (2017).

Abstract

Elucidating the factors that direct the spatio-temporal organization of evolving tissues is one of the primary purposes in the study of development. Various propositions claim to have been important contributions to the understanding of the mechanical properties of cells and tissues in their spatiotemporal organization in different developmental and morphogenetic processes. However, due to the lack of reliable and accessible tools to measure material properties and tensional parameters *in vivo*, validating these hypotheses has been difficult. Here we present methods employing atomic force microscopy (AFM) and particle tracking with the aim of quantifying the mechanical properties of the intact zebrafish embryo yolk cell during epiboly. Epiboly is an early conserved developmental process whose study is facilitated by the transparency of the embryo. These methods are simple to implement, reliable, and widely applicable since they overcome intrusive interventions that could affect tissue mechanics. A simple strategy was applied for the mounting of specimens, AFM recording, and nanoparticle injections and tracking. This approach makes these methods easily adaptable to other developmental times or organisms.

Video Link

The video component of this article can be found at https://www.jove.com/video/56224/

Introduction

The physical principles underlying the biomechanical control of morphogenetic processes are largely undefined. While biomechanical studies at the molecular and cellular level are gathering considerable momentum, the exploration of biomechanical parameters at the tissue/organism level is at its infancy. Hydrodynamic Regression[1] or Video Force Microscopy[2] allow researchers to distinguish active and passive forces, while laser microsurgery[3], or the less intrusive atomic force microscopy (AFM) of dissociated cells[4] or *in vivo*[5] or nanoparticle microrheology[6] allow the anticipation of a tissue's mechanical properties and responses.

AFM is a three-dimensional topographic technique with high atomic resolution resolving surface roughness and compliance from the deflection of cantilever tips upon contact with a probed surface[7]. Different methodologies employing AFM have been developed to investigate surface properties, including measuring friction, adhesion forces, and viscoelastic properties of diverse materials. Recently, AFM has emerged as a powerful tool to retrieve information on the mechanical properties of biological samples. In particular, AFM can non-invasively extract the complex shear modulus from single cells by applying oscillatory indentations with a micro tip attached to a cantilever of known bending constant[8]. This lets us infer resulting forces. Yet, AFM is not unique and different methodologies allow extracting rheological data and mechanical properties from individual cells (*e.g.,* Micropipette aspiration[9], magnetic twisting cytometry (MTC)[10], or uniaxial tensile testing[11]).

Yet, the application of these novel methodologies to complex morphogenetic processes is not straightforward. The main challenges faced when determining the mechanical properties of embryonic tissues are the small (µm to mm), soft (in the 10^2 - 10^4 Pa range) and visco-elastic (giving rise to time-dependent phenomena) nature of the material[12]. It is therefore important to adapt the methods employed for the determination of mechanical properties (stiffness, viscosity, adhesion) to the specific case of embryos and developing organisms. Two important issues need to be taken into consideration when analyzing rheological approaches to study development: to avoid intrusive interference and to provide easy accessibility. In this scenario, micropipette aspiration, MTC, and tensile testing exhibit limitations. In the first case, the high deformation that a cell suffers might alter its physiological and mechanical properties[9]. In the second case, the need to firmly adhere the experimental tissue to a substrate to ensure that the stresses applied deform the cytoskeleton locally could also introduce effects on the cells' activation state and, hence, in their mechanical features[10]. Last, uniaxial tensile approaches are limited by the geometry of developing organisms and accessibility[11].

AFM seems to be better suited for the study of developmental processes as it allows the study of biological samples directly in their natural environment without any cumbersome sample preparation. Moreover, as dissociation of embryonic tissues is generally difficult, the reduced size of AFM probes provides a high degree of versatility with no limitation in the choice of the type of medium (either aqueous or non-aqueous), sample temperature, or chemical composition of the sample. AFM is versatile enough to be applied to large domains and time scales and has been employed to retrieve material properties of tissues in distinct developmental stages or physiological conditions. Whole native tissues such as arteries[13] or bones[14] have been studied from a topographical point of view and in some cases, like the sclera, mechanical properties have also been retrieved[15]. Topography has also been explored in live embryos allowing the visualization of, for instance, cell rearrangement during

morphogenesis in Xenopus[16]. Last, comprehensive sample preparation protocols have been developed to determine mechanical parameters during different developmental processes. Nanoindentation maps have been generated on native unfixed tissue sections for the chick embryonic digestive tract[11]; adhesive and mechanical properties retrieved for individual ectoderm, mesoderm, and endoderm progenitor cells isolated from gastrulating zebrafish embryos[4]; stiffness measurements performed for the epiblast and primitive streak on explants from avian embryos[17]; and a distinct pattern of stiffness gradients directly defined in the embryonic brain of Xenopus[5].

A significant qualitative leap for applying AFM for exploring embryonic development may come from approaching simple accessible morphogenetic processes. Zebrafish epiboly is an essential and conserved event, in which different tissues coordinate in a restricted spherical space to direct the expansion of the blastoderm in a few hours. At the onset of zebrafish epiboly (spherical stage), a superficial layer of cells, the enveloping layer (EVL), covers a semi-spherical cap of blastomeres centered on the animal pole of the embryo sitting on a massive yolk syncytial cell. Epiboly consists of the cortical vegetal ward expansion of the EVL, the deep cells (DCs) of the blastoderm, and the external layer of the syncytial yolk cell (E-YSL) around the yolk. Epiboly ends with the closure of the EVL and the DCs at the vegetal pole[18,19,20]. How and where forces are generated during epiboly and how they are globally coupled is not yet clear[1,21].

Here we describe in detail how to apply AFM to infer passive mechanical tissue properties during epiboly progression in the zebrafish yolk cell *in vivo*. To do so, we employed small microspheres attached to AFM cantilevers as probes. This allows the retrieval of precise local information within the non-uniform yolk cell surface and to study tensional gradients and their dynamics over time. Alternative AFM approaches such as those using wedge cantilevers[22], will not render local data that is precise enough. The wedge technique, which requires very careful manipulation skills to glue a wedge larger than the sample size at the end of the cantilever, is not well suited for probing embryo (~2-fold larger than the length of the cantilever) mechanics.

Modeling and characterizing the viscoelastic properties of cells in qualitative and quantitative ways allows for an improved understanding of their biomechanics. From a biomechanical point of view, it is essential to understand epiboly, and not just demand knowledge on cortical tension measurements and dynamics, which can be extracted by AFM; thus there is need for information on the biophysical properties of the tissue. To extract this information, a variety of cell rheology techniques have been developed over the years in order to characterize different cell types under different physiological conditions[23]. They include AFM, MTC, and Optical Tweezers (OT). These methods, however, have been proven inadequate for mesoscopic analyses at the scale of embryos or organs. As an alternative, we have successfully adapted nanoparticle-tracking microrheology[6] for *in vivo* rheological measurements. This technique analyzes the Brownian displacements of individual particles and infers local micromechanical properties.

Together AFM and nanoparticle microrheology allow the definition of cortical tensional dynamics and internal mechanical properties of the yolk during epiboly. This information fully endorses a model in which anisotropic stress develops as a consequence of the differences in the deformation response of the EVL and the Yolk Cytoplasmic Layer (YCL) to the isotropic actomyosin contraction of the E-YSL cortex is essential for the directional net movement of the EVL and epiboly progression[1].

Protocol

All the protocol steps described below follow the animal care guidelines of our institutions.

1. Zebrafish Culture

1. Breed and maintain adult zebrafish under standard conditions.
   NOTE: AB and TL wild type embryos were used for this study.
2. Collect embryos and grow them at 28.5 °C in E3 embryo medium[24]. Stage them according to morphology as previously described[19].

2. Atomic Force Microscopy

1. Manually dechorionate staged zebrafish embryos (of different ages according to individual interests). Remove chorions with two thin and sharp forceps (see **Table of Materials**).
   1. Grip the chorion using one forceps and make a tear in it with the other forceps. Then, holding the chorion in a region opposite to that of the tear, push the embryo gently through the opening.
   2. Perform the dechorionation under a dissecting stereomicroscope with an adjustable range of magnification between 8X and 50X.

2. **Mount the embryos for AFM**
   1. Prepare a solution of 2% agarose in embryo medium and fill a 35-mm Petri dish with this. Let it solidify. Make small holes of 1.5 mm of diameter (twice the embryo size) and approximately 350 µm depth (half the embryo size) with thin forceps in the agarose bed.
   2. Place the embryos in the pokes made in the agarose layer and assure they are in place by spreading around a solution of 0.5% low melting agarose in embryo medium. Pour this solution around just the embryos to secure them in the holes.
   3. Before the low melting point agarose solidifies at room temperature, rotate the embryos in such a way that the region of interest to be probed by AFM will face upwards (**Figure 1A**).

3. **Examine the embryos by AFM**
   1. Locate and image the embryos in the petri dish employing a 20X objective in an Inverted Atomic Force Microscope (see **Table of Materials**[25]) at room temperature (23 - 24 °C).
      NOTE: The embryos are kept alive immersed in embryo medium and attached to the agarose bed.
   2. Probe the yolk cell surface of casted embryos employing spherical polystyrene beads of 4.5 µm in diameter attached to a cantilever with a nominal spring constant of 0.01 N/m. Set the peak-to-peak amplitude of cantilever oscillation to 5 µm and its frequency to 1 Hz.
   3. Collect data for each region to be tested in different positions and in several embryos, as a routine, for data averaging.

NOTE: A good starting point is to probe five positions located in the middle and at the corners of a 10 µm x 10 µm square by controlling the cantilever position with the XY piezo-actuators of the AFM microscope. Imaging and data collection took around 20 min per embryo. Recording data in different regions of the embryo yolk cell surface, *e.g.*, the vegetal pole or different regions close to the EVL cells margin (**Figure 1B** and **1C**), can only be done by employing distinct specimens oriented differently.

4. **Calculate forces**
   1. Measure the vertical displacement of the AFM cantilever (z) with strain gauge sensors coupled to piezo-actuators, and its deflection (d) using a quadrant photodiode by the optical lever method with the microscope control software (see **Table of Materials**[25]).
   2. Use the slope of a d-z curve obtained from data collected from a bare region of a glass coverslip to calibrate the correlation between the photodiode signal and the cantilever deflection (d).
      NOTE: The measured vertical displacement equals the cantilever deflection and the slope represents the deflection sensitivity of the optical lever[26].
   3. Infer the cantilever spring constant (*k*) from the thermal fluctuations as previously described[27].
   4. Compute the indentation of the sample (h) as:
      $h = (z - z_c) - (d - d_{off})$ (1)
      NOTE: Here z_c is the position of the contact point and d_{off} is the offset of the photodiode.
   5. Calculate the force (*F*) on the cantilever as:
      $F = k \cdot d$ (2)

5. **Calculate the tension of the cortex in terms of a liquid-balloon model consisting of an elastic layer of cortical tension T_c enclosing a viscous liquid. In this model, for small indentations (in comparison to the size of the embryo), force increases proportionally[4,28] as:**
   $F = 4\pi T_c [(R_b / R_e) +1)] h$ (3)
   NOTE: Here R_b is the radius of the bead and R_e is the radius of the embryo. For the zebrafish embryo, as the radius of the embryo (400 µm) is two orders of magnitude larger than that of the bead (2.25 µm), this equation can be approximated as:
   $F = 4\pi T_c h$ (4)
   1. Calculate the tension force-indentation (*F-h*) curves in each embryo yolk cell region for five different point measurements.
   2. Compute the T_c for each *F-h* curve by non-linear least-squares fitting. For statistical analysis, the cortical tension T_c computed must be averaged from the different *F-h* curves.

6. **Measure the viscoelastic properties (rheology) of the cortex by applying low amplitude (100 nm) multifrequency oscillations during AFM composed of sinusoidal waves of different frequencies[25].**
   1. Compute an effective complex modulus *g*(f)* in the frequency domain from the force indentation curves as:
      $g^*(f) = [F(f) / h(f)] - ifb$ (5)
      here *i* is the imaginary unit and *F*(*f*) and *h*(*f*) are the frequency (*f*) spectra of force and indentation. *b* is the correction for the viscous drag on the cantilever extracted from the oscillations applied on the surface.
   2. Separate *g*(f)* into real and imaginary parts as:
      $g^*(f) = g'(f) + ig''(f)$ (6)
      em>g'(*f*) is the elastic modulus and is a measure of the elastic energy stored and recovered per cycle of oscillation. *g*''(*f*) is the viscous modulus that accounts for the dissipated energy.
   3. Calculate the loss tangent, which provides an index of the solid-like (<1) or liquid-like (>1) behavior of the material, as:
      $g''(f) / g'(f)$ (7)
      NOTE: With this type of measurement, it is possible to extract parameters indicating how viscous and how elastic is the probed material. Although *b* slightly depends on the distance of the end of the cantilever to the surface, given the very low values of *g´´* exhibited by the yolk cell (see **Figure 2D** below), small variations in *b* have a negligible impact in the measurements[29].

3. Particle Tracking Microrheology

1. **Perform particle microinjection into the yolk cell**
   1. Fabricate tailored microneedles using a horizontal micropipette puller and borosilicate capillary glass (see **Table of Materials**).
      1. Prepare microneedles that have an outer diameter of 1.00 mm, an inner diameter of 0.58 mm and a length of 10 cm using puller settings: Pressure: 500; Heat: 510; Pull: 65; Velocity: 25; Time: 50.

   2. Prepare an injection petri dish plate by creating straight indentation lanes in a 1% agarose in embryo medium bed employing custom made molds (see **Table of Materials**).
      1. Turn the molds upside down and place them on top of the liquid agarose gel and remove the molds once the gel has solidified. Pipette the embryos into the grooves made by the mold in the agarose under a dissecting stereomicroscope at 1.2X magnification.
         NOTE: The width and design of the molds enable the embryos to self-align.

   3. Before injection, almost completely remove the medium to facilitate injection (the surface tension prevents the embryo/chorion from sticking to the needle when removing it after injection).
   4. Microinject fluorescent nanoparticles (radius a = 100 nm, see **Table of Materials**) diluted in water (1:1,000) in the vegetal part of the embryo yolk cell (**Figure 3A**).
   5. Adjust the micropipette with precision micromanipulators and inject the beads with an automatic microinjector with time and pressure controls (see **Table of Materials**). Set the pressure between 10 and 20 psi.
   6. Before injecting the bead solution, calibrate the volume to inject (0.5 nL) by measuring the droplet size delivered by the microinjector with a 1x 0.01 mm stage micrometer (see the **Table of Materials**).

7. Employ a magnification of 1.6X in the dissecting stereomicroscope to visualize the embryos during the injections, which are performed at room temperature.

2. **Assess the viscoelastic behavior of the yolk by recording thermal fluctuations**
   1. Dechorionate the microinjected embryos as in step 2.1 and embed them in a 0.5% low melting point agarose in embryo medium solution at 30 °C. Afterwards, transfer them to glass bottom plates (see **Table of Materials**) and orient and push them towards the coverslip when the agarose is still liquid.
      NOTE: When the agarose solidifies at room temperature, the embryos are ready to be imaged.
   2. Place the embryos mounted in the glass bottom plates on the stage of a confocal inverted microscope 2 h after microinjection. Capture images of the nanoparticles for 26 s at a sampling rate of 25 Hz with a 63X objective at room temperature in an inverted confocal microscope employing the standard commercial microscope software (pixel size = 166 nm, images captured every 40 ms).
   3. Compute the position of the particles' centroids and define their trajectories over time with the TrackMate plugin of the open source ImageJ software (**Figure 3B**).
   4. Calculate the two-dimensional Mean Square Displacement (MSD) of each particle with custom-made software[6,30] as:
      $\langle \Delta r^2(\tau) \rangle = \langle [x(t+\tau) - x(t)]^2 + [y(t+\tau) - y(t)]^2 \rangle$ (8)
      NOTE: Here t is the elapsed time and the time lag. In a pure viscous liquid, the MSD increases inversely with viscosity (v) according to the Stokes-Einstein relationship:
      $\langle \Delta r^2(\tau) \rangle = 4k_B T\tau / 6\pi v a$, (9)
      where T is the absolute temperature.

Representative Results

Cortical tension measurements
For each measurement point, five force-displacement (F-z) curves were acquired by AFM by ramping the cantilever at 1 Hz with a peak-to-peak amplitude of 5 µm (velocity = 10 µm/s) up to a maximum indentation of ~2 µm. This procedure was taking less than 20 min and was not affected by epiboly progression. Each experimental condition was tested in at least 5 embryos.

The force-displacement curves recorded on the embryo yolk cell, on the contrary to those corresponding to the soft surrounding agarose, exhibit a proportional linear relationship (R^2 >0.999) (**Figure 2A**). We performed additional sets of control F-z curves at 3 µm/s and 30 µm/s and discarded a potential dependence of cortical tension T_c on the velocity of the cantilever. T_c increased just by 13% ($p < 0.01$, t-test) when the velocity was reduced from 10 to 3 µm/s and did not show any significant change when increased from 10 to 30 µm/s.

Force-indentation (F-h) curves recorded at a cantilever velocity of 10 µm/s on the yolk cell were almost linear and fitted with a liquid-balloon model (**Figure 2B**)[1]. This fitting allowed the calculation of the absolute values of mean surface tension (pN/µm) at different epiboly stages and at different positions relative to the EVL leading edge (identified under transmitted light) (**Table 1**).

Rheology of the cortex
The differences between the indentation and retraction of force-displacement (F-z) curves (**Figure 2C**) indicate a viscoelastic behavior of the embryo yolk cell cortex. Low amplitude (100 nm) multifrequency oscillation measurements provide the information to calculate the effective complex modulus $g^*(f)$ of the yolk cell surface and its elastic and viscous components (see protocol above).

The cortex rheology in the zebrafish embryo yolk cell is dominated by a solid-like behavior with the viscous modulus 5 times lower than the elastic modulus[1]. This behavior is not frequency dependent, either for the elastic (ANOVA, $p = 0.123$), or for the viscous modulus (ANOVA, $p = 0.719$) (**Figure 2D**).

Rheology of the yolk
The viscosity of the yolk was computed by fitting equation (5) to the MSD data obtained from nanoparticle tracking (see **Figure 4A-B**). The MSD of thermal fluctuations of fluorescent nanoparticles embedded in the yolk exhibits a proportional dependence on time lag τ, consistent with the behavior of a Newtonian liquid. The effective shear viscosity of the yolk, which is inversely related to the bulk diffusion coefficients of the nanoparticles, was 129 mPa·s.

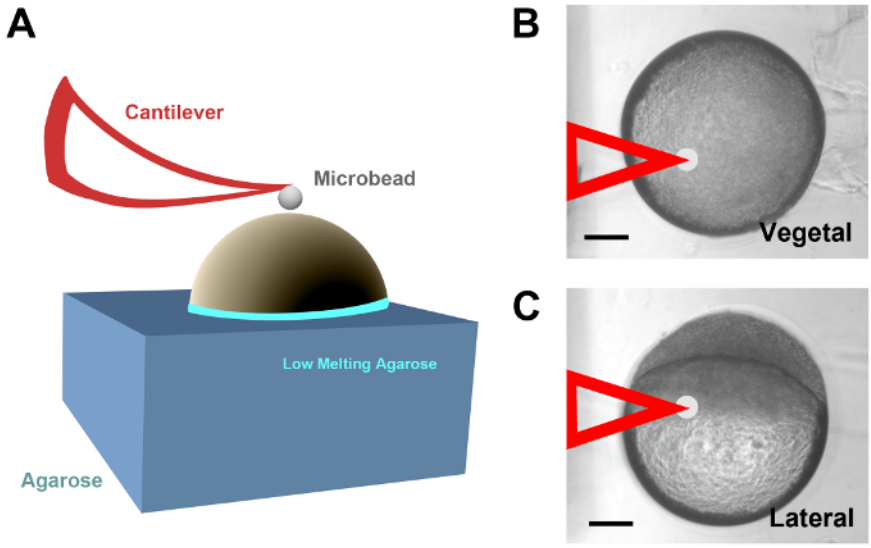

Figure 1: AFM of zebrafish yolk cells *in vivo*. (A) Diagram describing the set up employed to probe the zebrafish yolk cell cortex by AFM. Dechorionated embryos of different ages were halfway inserted into holes created in customized agarose blocks, rotated into a particular orientation and sealed at the edges with low melting point agarose. The yolk cells were probed with spherical polystyrene beads attached to a cantilever (red). **(B)** Embryo at 50% epiboly half embedded in agarose probed with a cantilever (false colored in red) at the vegetal pole. **(C)** An equivalent embryo to that in **B**, probed at the yolk cell in a region close to the EVL cells margin. Scale bars = 100 µm (B and C). Please click here to view a larger version of this figure.

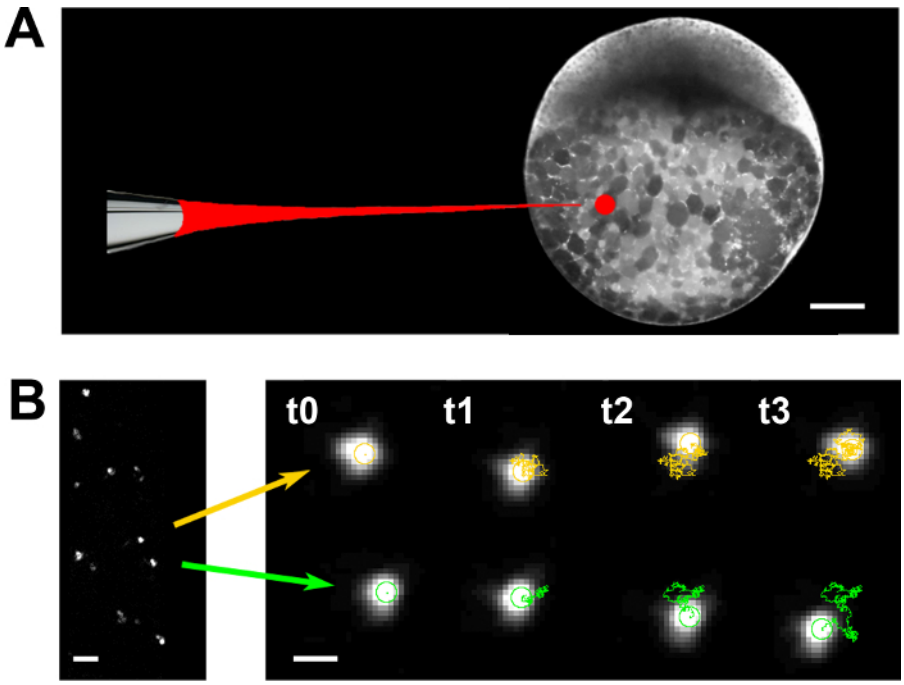

Figure 2. Zebrafish embryo yolk cell cortical tension and rheology. (A) Force [deflection (d)]-displacement (z) curves obtained for a representative embryo as the cantilever tip approaches and contacts the sample [the agarose surface (control) in blue and the yolk cell surface in red]. **(B)** Force indentation (F-h) curves (n = 3 embryos, 3 measurements per embryo at a distance of 10 µm from each other. Each measurement represents the mean of 5 curves) fit with a liquid-balloon model (from reference[1]). Note the linear increase in deflection upon contact with the embryo yolk cell surface. The dashed black line shows the fitting to the model (from which the cortical tension is inferred). **(C)** Approximation (red) and retraction (purple) force-displacement curves for a representative embryo. Curved red and purple arrows point to the temporal regime of data collection. The double-headed arrow highlights the difference between the approaching and retracting deflection values pointing to the viscoelastic character of the cortex. **(D)** Viscoelasticity of the yolk cell cortex (n = 5 embryos). Effective complex modulus (g*) extracted from multifrequency oscillations AFM measurements (from [1]). Red symbols represent the elastic modulus (g'), and blue symbols define the viscous modulus (g″), respectively. Mean and Standard Error (SE) are displayed. Please click here to view a larger version of this figure.

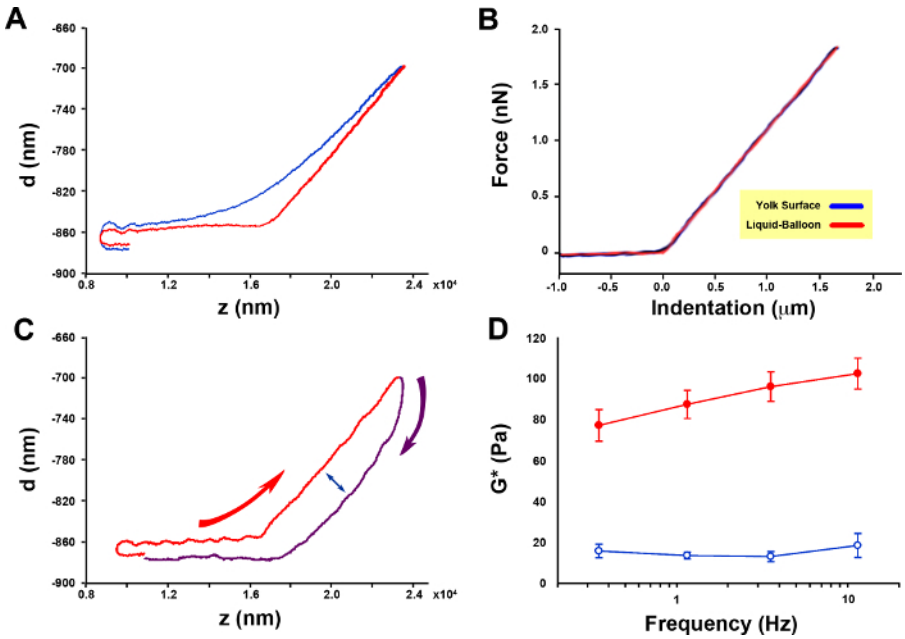

Figure 3. Particle tracking microrheology. (A) Fluorescent nanoparticles are injected into the yolk cell of zebrafish embryos at 50% epiboly. **(B)** Displacements were tracked for individual nanoparticles randomly distributed within the yolk (left). Time course of the typical trajectories of nanoparticles (centroids) embedded within the yolk (2 examples) exhibit random walks that are characteristic of viscous diffusion. Scale bar = 100 μm (A); 1 μm (B, left); 200 nm (B, right). Please click here to view a larger version of this figure.

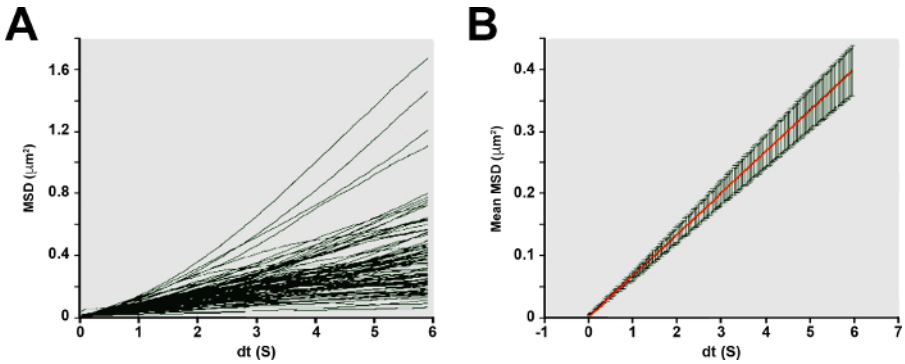

Figure 4. Microrheology of the zebrafish embryo yolk. (A) MSDs of individual nanoparticles (n = 99) exhibit an approximately linear dependence with time lag. **(B)** Mean ± standard error MSDs of nanoparticles and viscosity of the yolk. Ensemble averaged MSDs (mean - red line ± SE) of the nanoparticle population exhibits predominantly viscous character. The linear slope of the relationship reflects the diffusive properties of the nanoparticles. Please click here to view a larger version of this figure.

Tension (pN/mm) Average ± SE		**% of Epiboly**		
		40-50	**60-70**	**80-90**
Distance to EVL margin	**20 μm (E-YSL)**	-	60 ± 7	-
	40 μm (YCL)	67 ± 11	72 ± 5	110 ± 7
	Vegetal Pole	-	75 ± 3	-
n = 3 embryos (5 indentations on each) for each condition				

Table 1: Spatio-Temporal Tension distribution at the yolk cell surface during Epiboly.

Discussion

Here we show that the material properties and some biomechanical parameters of the zebrafish yolk cell during epiboly can be readily estimated by AFM and nanoparticles microrheology.

While AFM has been employed to retrieve rheological features of cells and tissues in physiological conditions[4,5,25,28], here we developed a protocol for applying AFM to intact developing embryos that we employed to test the yolk cell surface of the zebrafish embryo during epiboly.

For our AFM measurements, the orientation of the embryos was secured by half embedding them in low melting agarose. Yet, agarose embedding did not affect AFM measurements. The stiffness of the agarose was measured by probing its surface with a spherical tip. We found a Young's modulus (*E*) of 4.2 0.2 Pa for this gel by fitting the force-indentation curves with the Hertz contact model of a sphere indenting a flat surface of an elastic body. Given that *E* 3*g*', the agarose was 50-fold softer than the yolk cell cortex (**Figure 2D**). Therefore, considering its limited thickness and very low stiffness, the AFM measurements recorded atop the embryo appear to be extremely reliable.

It is important to note that retrieving absolute values for cortical tension from AFM data demands extreme care on regarding mechanical model fitting. In the case of the zebrafish yolk cell, with its unique composition with an outer microtubules-rich cytoplasmic layer encompassing a highly viscous yolk mass, we circumvent this problem employing a liquid-balloon model consisting of an elastic cortex enclosing a viscous liquid. This model has been previously used to estimate the cortical tension of leucocytes with micropipette aspiration[28], spherical progenitor cells from gastrulating zebrafish embryos indented with spherical AFM tips[4], and HeLa cells with AFM using wedged cantilevers[22].

We estimated the cortical tension of the yolk cell by indenting its surface with a commercially available small spherical tip. This small probe allowed us to directly measure regional differences in cortical tension. As described above, force-indentation data were interpreted in terms of a minimal liquid-balloon model (Eq. 2). Force curves recorded on the surface of gels and cells with a spherical tip increase with indentation as a power law with a 3/2 exponent. By contrast, we found a proportional force-indentation relationship very well fitted with Eq. 2 (**Figure 2B**). The little dependence of T_c on cantilever velocity and the low *g*''/*g*' ratio (**Figure 2D**) indicates that cortex mechanics is dominated by an elastic behavior.

Yolk mechanics were independently probed with microparticle rheology. The linear increase of MSD observed clearly reflects a pure viscous behavior. It should be noted that the viscosity of polymer solutions depends on the size of the probe[31]. Therefore, the value of yolk viscosity we measured with a probe of 100 nm in radius could somewhat differ from molecular (*e.g.*, fluoresce depolarization) or macroscopic measurements. Taken together, these results provide strong support to the adequacy of the liquid-balloon model and the robustness of the cortical tension and yolk viscosity measurements.

We reason that this approach could be easily extended to measure blastoderm mechanics in the same embryos or to other developmental time points in the zebrafish and, eventually, to other organisms. This approximation will only depend on engineering appropriate mounting procedures (see reference[32]) facilitating the access of the AFM probes to the right places at the right time. Still, the continuous motion of most cells and tissues during development should be taken into account in any application to other developmental models. Cell movements will make the application of these methods much more challenging.

In some cases, AFM *in vivo* would be inapplicable if accessibility problems cannot be overcome. Both in developing embryos and adults, cells are largely inaccessible. Thus, to test biophysical properties *in situ*, is imperative to employ methods not requiring direct contact. Nanoparticle tracking microrheology fulfills these requirements[6]. This technique is based on the analysis with high spatial and temporal resolution of the Brownian displacements of individual particles. The local micromechanical properties of the viscoelastic fluid that surrounds these nanoparticles is a direct reflection of the extent and time lag-dependence of their MSDs. This approach has already been applied to developing organisms and has helped to determine the highly viscous character of the *C. elegans* embryo cytoplasm[30]. We uncovered that a zebrafish yolk displays equivalent properties with C. *elegans* embryos, although its viscosity is two orders of magnitude lower. A linear time dependence of MSD with similar values of yolk viscosity to those of the zebrafish yolk has recently been reported in *Drosophila*[33].

Although we did not explore this possibility ourselves, injected uncoated and coated nanoparticles have recently been employed as targets of optical tweezers in zebrafish larvae[34]. Non-invasive micromanipulation inside a whole-organism may give not just direct insights into cell interactions but into mechanical properties and activities not accessible using existing approaches.

Disclosures

The authors declare no competing financial interests or other conflicts of interest.

Acknowledgements

We thank Amayra Hernández-Vega and Philippe-Alexandre Pouille for participating in setting up the basis for these protocols. We also thank the Molecular Imaging Platform from the IBMB-PCB, Xavier Esteban and members of the laboratory for continuous support. The Consolidated Groups Program of the Generalitat de Catalunya and DGI and Consolider Grants from the Ministry of Economy and Competitivity of Spain to EMB and DN supported this work.

References

1. Hernandez-Vega, A. *et al.* Polarized cortical tension drives zebrafish epiboly movements. *EMBO J.* **36**, 25-41 (2017).
2. Brodland, G. W. *et al.* Video force microscopy reveals the mechanics of ventral furrow invagination in Drosophila. *Proc Natl Acad Sci U S A.* **107**, 22111-22116 (2010).
3. Grill, S. W. Growing up is stressful: biophysical laws of morphogenesis. *Curr Opin Genet Dev.* **21**, 647-652 (2011).
4. Krieg, M. *et al.* Tensile forces govern germ-layer organization in zebrafish. *Nat Cell Biol.* **10**, 429-436 (2008).
5. Koser, D. E. *et al.* Mechanosensing is critical for axon growth in the developing brain. *Nat Neurosci.* **19**, 1592-1598 (2016).
6. Wirtz, D. Particle-tracking microrheology of living cells: principles and applications. *Annu Rev Biophys.* **38**, 301-326 (2009).
7. de Pablo, P. J., & Carrión-Vázquez, M. Imaging Biological Samples with Atomic Force Microscopy. *Cold Spring Harbor Protocols.* **2014**, 167-177 (2014).
8. Roca-Cusachs, P. *et al.* Rheology of passive and adhesion-activated neutrophils probed by atomic force microscopy. *Biophys J.* **91**, 3508-3518 (2006).

9. Evans, E., & Yeung, A. Apparent viscosity and cortical tension of blood granulocytes determined by micropipet aspiration. *Biophys J.* **56**, 151-160 (1989).
10. Fabry, B. *et al.* Time scale and other invariants of integrative mechanical behavior in living cells. *Phys Rev E Stat Nonlin Soft Matter Phys.* **68**, 041914, (2003).
11. Kashef, J., & Franz, C. M. Quantitative methods for analyzing cell-cell adhesion in development. *Dev Biol.* **401**, 165-174 (2015).
12. Chevalier, N. R. *et al.* Measuring the micromechanical properties of embryonic tissues. *Methods.* **94**, 120-128, (2016).
13. Reichlin, T. *et al.* Investigating native coronary artery endothelium in situ and in cell culture by scanning force microscopy. *J Struct Biol.* **152**, 52-63 (2005).
14. Rho, J. Y., Tsui, T. Y., & Pharr, G. M. Elastic properties of osteon and trabecular bone measured by nanoindentation. *J Biomech.* **31**, 21, (1998).
15. Grant, C. A. *et al.* Surface characterisation and biomechanical analysis of the sclera by atomic force microscopy. *J Mech Behav Biomed Mat.* **4**, 535-540 (2011).
16. Efremov, Y. M. *et al.* Atomic force microscopy of living and fixed Xenopus laevis embryos. *Micron.* **42**, 840-852 (2011).
17. Henkels, J. *et al.* Spatiotemporal Mechanical Variation Reveals Critical Role for Rho Kinase During Primitive Streak Morphogenesis. *Ann Biomed Eng.* **41**, 421-432 (2013).
18. Solnica-Krezel, L. Gastrulation in zebrafish -- all just about adhesion? *Curr Opin Genet Dev.* **16**, 433-441 (2006).
19. Kimmel, C. B. *et al.* Stages of embryonic development of the zebrafish. *Dev Dyn.* **203**, 253-310 (1995).
20. Rohde, L. A., & Heisenberg, C. P. Zebrafish gastrulation: cell movements, signals, and mechanisms. *Int Rev Cytol.* **261**, 159-192 (2007).
21. Campinho, P. *et al.* Tension-oriented cell divisions limit anisotropic tissue tension in epithelial spreading during zebrafish epiboly. *Nat Cell Biol.*, **15**, 1405-1414 (2013).
22. Fischer-Friedrich, E. *et al.* Quantification of surface tension and internal pressure generated by single mitotic cells. *Sci Rep.* **4**, 6213 (2014).
23. Moeendarbary, E., & Harris, A. R. Cell mechanics: principles, practices, and prospects. *Wiley Interdiscip Rev Syst Biol Med.* **6**, 371-388 (2014).
24. Westerfield, M. *The Zebrafish Book: A Guide for the Laboratory Use of Zebrafish (Danio rerio).* Eugene, OR: University of Oregon Press (2000).
25. Alcaraz, J. *et al.* Microrheology of human lung epithelial cells measured by atomic force microscopy. *Biophys J.* **84**, 2071-2079 (2003).
26. Jorba, I. *et al.* Probing Micromechanical Properties of the Extracellular Matrix of Soft Tissues by Atomic Force Microscopy. *J Cell Physiol.* **232**, 19-26 (2017).
27. Hutter, J. L., & Bechhoefer, J. Calibration of atomic-force microscope tips. *Review of Scientific Instruments.* **64**, 1868-1873 (1993).
28. Lomakina, E. B. *et al.* Rheological analysis and measurement of neutrophil indentation. *Biophys J.* **87**, 4246-4258 (2004).
29. Alcaraz, J. *et al.* Correction of Microrheological Measurements of Soft Samples with Atomic Force Microscopy for the Hydrodynamic Drag on the Cantilever. *Langmuir.* **18**, 716-721 (2002).
30. Daniels, B. R., Masi, B. C., & Wirtz, D. Probing single-cell micromechanics in vivo: the microrheology of C. elegans developing embryos. *Biophys J.* **90**, 4712-4719 (2006).
31. Kalwarczyk, T. *et al.* Comparative analysis of viscosity of complex liquids and cytoplasm of mammalian cells at the nanoscale. *Nano Lett.* **11**, 2157-2163 (2011).
32. Soroldoni, D. *et al.* Genetic oscillations. A Doppler effect in embryonic pattern formation. *Science.* **345**, 222-225 (2014).
33. He, B. *et al.* Apical constriction drives tissue-scale hydrodynamic flow to mediate cell elongation. *Nature.* **508**, 392-396 (2014).
34. Johansen, P. L. *et al.* Optical micromanipulation of nanoparticles and cells inside living zebrafish. *Nat Commun.* **7**, 10974 (2016).

